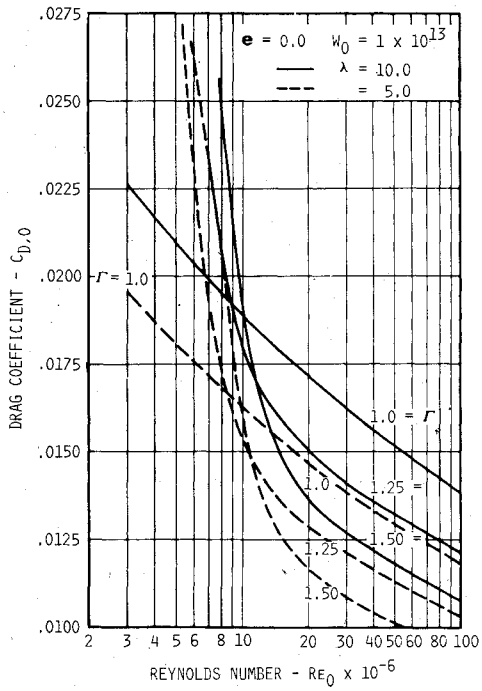

Fig. 1 Influence of vehicle density and fineness ratio on the nominal drag coefficient.

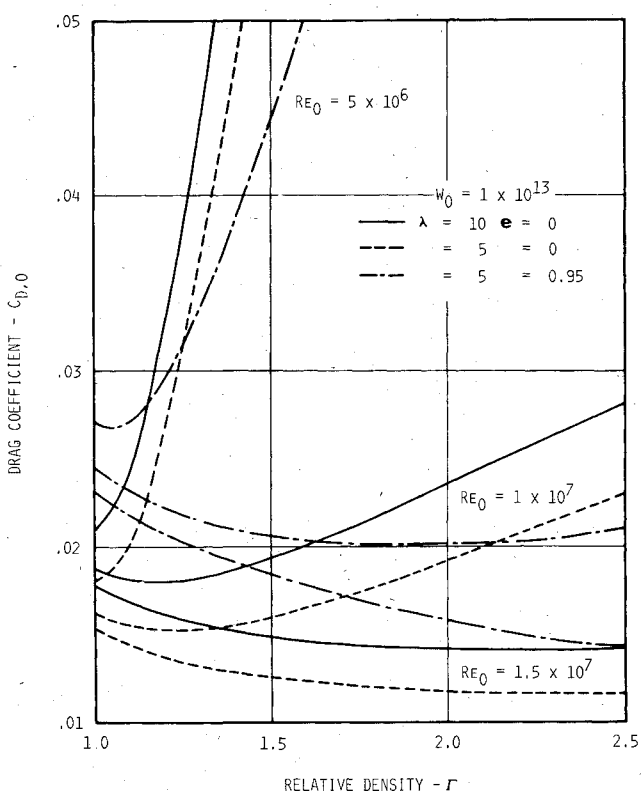

Fig. 2 Variation of the nominal drag coefficient with the vehicle density.

coefficient of a neutrally buoyant vehicle of equal mass. Representative results of parametric studies are shown in Figs. 1 and 2.

Results and Conclusions

The principal parameters in this study are the relative density Γ, the cross section eccentricity e, the fineness ratio λ, the Reynolds number Re_0, and the size W_0. Variation of the drag coefficient $C_{D,0}$ with the Reynolds number of a Γ = 1 vehicle of identical mass is shown in Fig. 1. Effectiveness of the use of lift can be evaluated directly by comparing the results with those for Γ = 1. The lifting vehicles are smaller and despite the larger skin friction coefficients have lower total skin friction drag due to the smaller size, but suffer from the effects of induced drag. It is clear that at low Reynolds numbers, the induced drag resulting from high angle-of-attack operation overwhelms the reduction of frictional drag and lifting vehicles are ineffective. At very high Reynolds numbers, the angles of attack are very small and the reduction in drag is due mainly to the smaller size. The significant benefits which can be realized from lower fineness ratios are clearly brought out. When the drag coefficient is plotted against the relative density in Fig. 2, it is seen that the minima exist in most cases at relatively modest values of Γ. The preliminary results exhibited here indicate that significant reductions in drag can be achieved through the use of dense vehicles employing lift. Considerable further gains could be realized through the use of more efficient lifting configurations.

References

[1] Lauchle, G. C., Eisenhuth, J. J., and Gurney, G. B., "Boundary Layer Transition on a Body of Revolution," *Journal of Hydronautics*, Vol. 14, Oct. 1980, pp. 117-121.

[2] Hoerner, S. F., *Fluid Dynamic Lift*, published by the author, Brick Town, N.J., 1975, Chaps. 17 and 19.

[3] Goldstein, S., ed., *Modern Developments in Fluid Dynamics*, Oxford University Press, London, 1938, Vol. II, Chap. XI, p. 509.

AIAA 81-0181R

Measurements of Conditioned Velocities in a Turbulent Premixed Flame

I. G. Shepherd* and J. B. Moss†
The University of Southampton, Southampton, England

Introduction

IT is customary when modeling turbulent fluxes in chemically reacting flows to use gradient or eddy viscosity formulations developed by analogy with those appropriate to cold flows. However, Libby and Bray[1] recently have pointed out that in weakly sheared ("normal") premixed flames the eddy transport mechanism is unsuitable and they propose an alternative closure avoiding gradient assumptions. To date there have been insufficient time-resolved data available from flames to test adequately such modeling hypotheses. Recent developments in the determination of scalar properties in conjunction with laser Doppler anemometry (LDA) permit increasingly detailed comparisons between model and experiment.

A knowledge of the joint probability density function for velocity and concentration is crucial to the alternative strategies for modeling the turbulent diffusion of species, $\rho u'' c''$, for example. Simplification of this pdf results if local burning zones are thin and, in consequence, the mixture states

Presented as Paper 81-0181 at the AIAA 19th Aerospace Sciences Meeting, St. Louis, Mo., Jan. 12-15, 1981; submitted Feb. 24, 1981; revision received Sept. 2, 1981.

*Research Fellow, Dept. of Aeronautics and Astronautics.
†Lecturer, Dept. of Aeronautics and Astronautics.

are predominantly either unburnt or fully burnt.[2] Concentration entries in the pdf are then confined to the planes $c=0$ and $c=1$. Measurements reported by Yoshida and Guenther[3] using fine wire thermocouples, and Moss[4] using light scattering from an inert particle seed, confirm that the scalar pdf has this simplified form in open turbulent premixed flames.

The present Note describes a technique for the joint determination of velocity, using LDA, and density, using the light scatter from the same measurement volume. By incorporating the thin flame notion directly into the procedures for data analysis, the density determination is simplified to that of generating a scalar conditioning function which permits the two scalar states, burnt gas and unburnt mixture, to be distinguished.

Recent extensions to the Bray-Moss-Libby model of premixed turbulent combustion,[1,5] employing a fast chemistry assumption to decompose the joint pdf for velocity u and reaction progress variable c, lead to simple expressions for the Favre-averaged mean turbulent flux

$$\overline{\rho u'' c''} = \bar{\rho}\tilde{c}(1-\tilde{c})(\tilde{u}_p - \tilde{u}_r) \qquad (1)$$

and intensity of velocity fluctuations

$$\overline{\rho u''^2}/\bar{\rho} = \tilde{c}(1-\tilde{c})(\tilde{u}_p - \tilde{u}_r)^2 + (1-\tilde{c})\overline{u_r'^2} + \tilde{c}\,\overline{u_p'^2} \qquad (2)$$

in terms of conditioned statistics; r denoting values in unburnt reactant mixture and p in fully burnt reaction product. ρ is the mixture density. These statistics are readily determined by the technique described here.

Experimental Detail

A rich premixed propane/air flame (flow velocity 2.8 ms^{-1}, equivalence ratio 1.6, and 11% turbulence at the exit plane of the burner) was stabilized on the water-cooled rim of a 5-cm-diam pipe. The flow conditions were selected in order to satisfy the narrow range of approach flow velocities and equivalence ratios which could be readily rim-stabilized without the use of a pilot flame and also permit as large an included angle for the premixed flame cone as possible. Thus a more nearly normal configuration was sought with possibly smaller Reynolds shear-stress contributions to turbulent processes than some other recently reported studies.[6,7] The air flow was seeded with dry TiO_2 powder ($\sim$1-μm nominal diam) introduced from a cyclone generator.[8] The light scattered by the particles on passage through the LDA fringe field was collected by a conventional lens system and photomultiplier tube. The Doppler signals were processed by a tracking filter which produces a voltage directly proportional to the Doppler frequency and, hence, to the instantaneous velocity.

Seeding with dry powders has been and remains one of the central problems in the application of LDA techniques to combusting systems. The LDA seeding requirements may be summarized as follows.

1) The particles must be small enough to faithfully follow fluctuations in flow velocity within the frequency range of interest.

2) A high seed density is necessary to eliminate tracker signal dropout.

3) If the same scattered light signal is to provide density information in premixed flames the mean scattered intensities from burnt and unburnt gas must be sufficiently distinguishable for the states to be discriminated.

4) Hence there should be a steady seeding rate to avoid ambiguity between these states.

Figures 1a-c present typical unprocessed data obtained from the pm tube and the tracker for the two inert seed materials considered here: TiO_2 and Al_2O_3. Both are dry powders though the Al_2O_3 particles are typically larger than those of TiO_2. Signal dropout is evident in the comparison of

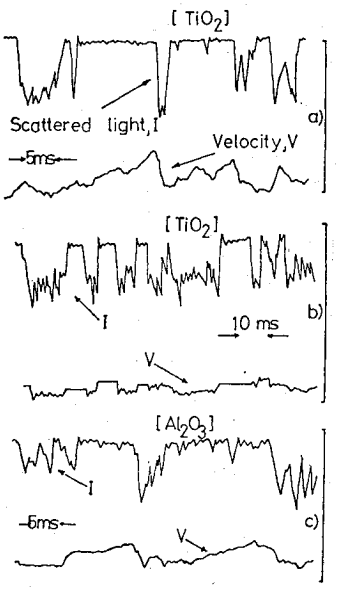

Fig. 1 Typical light intensity and velocity time histories.

Fig. 1a for a heavily seeded flow, with Fig. 1b, a lightly seeded case. Although both scattered light records would allow ready discrimination between burnt (the upper level) and unburnt states, in Fig. 1b "flats" appear in the velocity record due to dropout. In the absence of signal the tracker holds the last voltage level processed. This is a more serious problem in the burnt gas where, due to heat release, there is a much lower particle number density. A continuous velocity record is obtained with Al_2O_3 but problems of level discrimination can arise, cf. Fig. 1c. This is due to high-marker shot noise associated with a relatively small decrease in mean scattered light intensity on passage through the flame. An $\sim$6 fold decrease is observed here compared with $\sim$20 fold for TiO_2 enhanced by changes in scattering properties.[9] With the latter, the fluctuations in seeding level, which seem inevitable with aerodynamic particle generators, then rarely exceeded acceptable levels from the standpoint of discrimination and few records with TiO_2 had to be rejected. The preceding considerations led to the adoption of TiO_2 as the seed material throughout the present study. The heavy seeding levels required by the tracker to overcome dropout, in comparison with, say, processing via a counter, made it possible to obtain velocity and scattered light intensity from the same pm tube using the same sampling volume. The key features of the present technique thus lie in improvements in signal processing of both the LDA and of the less stringent requirement on the scalar measurement if only a conditioning function is sought. This approach is a significant advance on the combined concentration and velocity measurements recently reported by Moss[4] which had to employ separate collection optics and compromised spatial resolution. The present seeding requirements did, however, prohibit the use of a seed generator producing TiO_2 particles from the reaction between $TiCl_4$ and moist air.[4,9] Though the seeding so produced is dense and more uniform than that from dry powder devices, the accompanying HCl is unacceptable within the confines of the laboratory.

Results and Discussion

Data were obtained from a vertical traverse parallel to and 1.5 cm from the burner axis. Since the scalar pdf essentially comprises two delta functions corresponding to unburnt and burnt gas, a simple analogue device with a variable voltage discriminator was used to regenerate the assumed square wave for gas density, i.e., removing marker shot noise from the scattered light signal. The signal was then used to gate the continuous velocity record, so identifying contributions from these two states. From the velocity time series, conditioned in

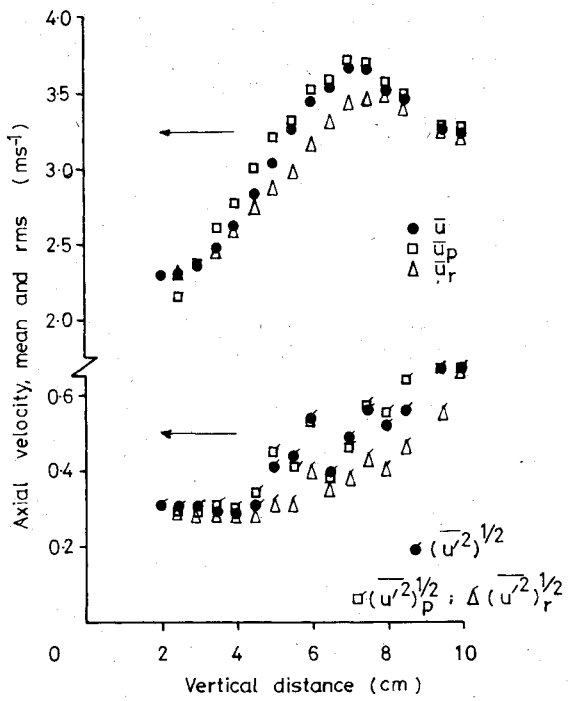

Fig. 2 Profiles of mean and rms vertical velocity.

this way, it was possible to build up pdf's of the velocities of the burnt and unburnt states throughout the flame. Conditioned mean and rms velocities were then derived by integration. The variations through the flame are shown in Fig. 2.

Important features of the distribution in Fig. 2 are 1) the mean velocity in the burnt gas, $\bar{u}_p$, is significantly larger than that in the unburnt mixture, $\bar{u}_r$, throughout; 2) the intensity of the velocity fluctuations increases in passing from unburnt to burnt gas; and 3) in general, the measured intensity in the burnt gas exceeds that in unburnt mixture.

The implications of these results for turbulence modeling will be briefly reviewed and, in particular, the data presented in a form permitting comparison with the recent work of Libby et al.[1,5] for normal flames. The vertical distance is transformed into the progress variable using the measured scattered light profile to determine mean density, and the measured vertical velocities are transformed into the component normal to the mean flame position following the procedure adopted by Bray et al.[5] The flame cone included angle was 19 deg in the present study. In view of the large streamline deflection observed through unconfined flames, this latter transformation introduces considerable uncertainty in the absolute values and more detailed mapping of the flowfield in joint velocity-density space must include measurements of the orthogonal velocity components.

The normal eddy viscosity assumption models the turbulent species flux as

$$\overline{\rho c'' u''} = -\bar{\rho} \nu_T \frac{\partial \tilde{c}}{\partial x} \tag{3}$$

with u, x positive in the direction of flow. However, since the gradient $\partial\tilde{c}/\partial x$ is positive on passage through the flame, Eqs. (1) and (3) cannot be reconciled if, as observed, $\bar{u}_p > \bar{u}_r$. The turbulent diffusion thus takes place in the opposite direction to that predicted by Eq. (3). The counter-gradient turbulent flux, normal to the flame, is illustrated in Fig. 3, together with the Favre-averaged turbulence intensity, evaluated from the conditioned moments normal to the flame as described by Eq. (2). The measured turbulence intensity increases through the flame zone, supporting suggestions[1,5] that in weakly-sheared flames turbulence production by the small self-induced mean

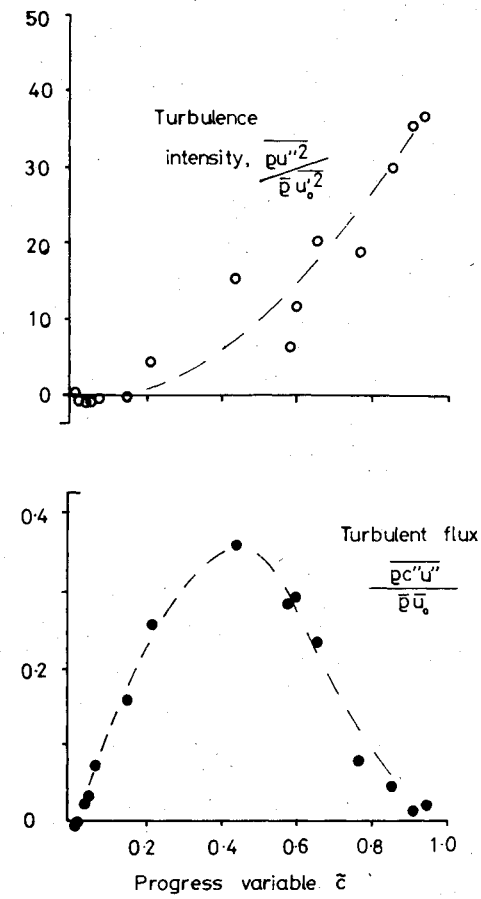

Fig. 3 Favre-averaged turbulent flux and turbulence intensity normal to the flame.

pressure gradient overwhelms the effects of dilatation due to heat release which would tend to reduce turbulence levels. That there is no indication of any reduction in turbulence intensity in the postflame region is surprising. The explanation would seem to lie in the extensive outflow through the broadly conical flame surface in the open burner configuration. The traverse parallel to the burner axis does not follow a mean streamline and the postflame measurements are made in gas which burnt in the disturbed region near the apex of the flame cone.

Conclusions

1) A novel technique is described for determining conditioned velocity information in premixed flames.

2) A tracking filter with its heavy seeding requirements offers very considerable advantages over lightly seeded alternatives, for example, counting procedures in combined measurements of velocity and concentration.

3) The measurements afford a unique insight into the prevailing mechanisms and turbulence structure, revealing in counter-gradient diffusion important shortcomings in conventional gradient modeling.

Acknowledgment

This work is partly supported by the United States Air Force under Grant AFOSR-79-0049.

References

[1] Libby, P. A. and Bray, K.N.C., "Counter-Gradient Diffusion in Premixed Turbulent Flames," *AIAA Journal*, Vol. 19, Feb. 1981, p. 205-213.

[2] Bray, K.N.C. and Moss, J. B., "A Unified Statistical Model of the Premixed Turbulent Flame," *Acta Astronautica*, Vol. 4, 1977, pp. 291-319.

[3]Yoshida, A. and Guenther, R., "Temperature and Ionization Measurements in Turbulent Premixed Flames," AIAA Paper 80-0207, Jan. 1980.
[4]Moss, J. B., "Simultaneous Measurements of Concentration and Velocity in an Open Premixed Turbulent Flame," *Combustion Science and Technology*, Vol. 22, 1980, p. 115.
[5]Bray, K.N.C., Libby, P. A., Masuya, G., and Moss, J. B., "Turbulence Production in Premixed Turbulent Flames," *Combustion Science and Technology*, Vol. 25, 1981, pp. 127-140.
[6]Yoshida, A. and Tsuji, H., "Measurements of Fluctuating Temperature and Velocity in a Turbulent Premixed Flame," *Proceedings of the 17th Symposium (International) on Combustion*, Combustion Institute, 1979, p. 945.
[7]Yanagi, T. and Mimura, Y., "Velocity-Temperature Correlation in a Premixed Flame," Paper presented at 18th Symposium (International) on Combustion, Waterloo, Canada, 1980.
[8]Glass, M. and Kennedy, I. M., "An Improved Seeding Method for High Temperature Laser Doppler Velocimetry," *Combustion and Flame*, Vol. 29, 1977, pp. 333.
[9]Kennedy, I. M., "Scalar Measurements in Turbulent Diffusion Flames," Ph.D. Thesis, University of Sydney, Sydney, Australia, 1979.

AIAA 82-4100

Porous Plate Analog Burner Study of Composite Solid Propellant Flame Structure

L. D. Strand* and N. S. Cohen†
Jet Propulsion Laboratory,
California Institute of Technology, Pasadena, Calif.

A POROUS plate burner apparatus was applied to study the structure and interaction of diffusion flames from unlike adjacent sources (size or type) of oxidizer under conditions simulating those of composite solid propellants. The burner provides diagnostic flexibilities not available with solid propellants—expanded spatial and temporal characteristics to afford accurate resolution of the flames, and geometric and stoichiometric combinations not processible in actual solid propellants.

The details of the burner (Fig. 1) have been published previously.[1,2] Metered hydrocarbon gases are passed through the porous plate to represent binder decomposition. Oxidizer gases pass through ports of selectable diameter and arrangement inserted in the porous plate, representing decomposing oxidizer crystals. The gases mix to create a diffusion flame representative of composite propellant combustion. The porous plate and port arrangement is enclosed in a windowed pressure vessel.

New porous plates and manifolding were fabricated for this program (Fig. 2). The port sizing and arrangements were based upon considerations of data acquisition, ease of fabrication, simulation, oxidizer-to-fuel (O/F) ratios to be achieved, flow rates, gas velocities, and Reynolds numbers, making use of Ref. 1 experience. The plates were designed to simulate monomodal and bimodal oxidizer composite propellants, and the manifolding afforded independent flow control for each size mode and/or the use of two different oxidizer gases. The gases used in these tests were ethane, air, oxygen, and oxygen-air mixtures. Independent variables were flow rate, O/F ratio, and pressure. Diffusion flame structures were observed visually and photographically. Examples of photographs acquired are shown in Figs. 3a-c.

Received Aug. 3, 1981.

*Member of Technical Staff. Associate Fellow AIAA.
†Contractor, Cohen Professional Services. Member AIAA.

Discussion of Results

The most interesting results were acquired with the bimodal oxidizer porous plates. At highest oxidizer flow rates, the coarse port flames tended to bend toward the fuel (i.e., away from the ports), whereas the fine port flames were columnar in nature. This indicates that the coarse ports were oxidizer rich, whereas the fine ports were near stoichiometric.[3] At lower oxidizer flow rates, the coarse port flames became columnar, whereas the fine port flames began to bend toward the oxidizer port centerlines and eventually close over them (forming a parabolic flame). This indicates that the coarse ports were near stoichiometric and the fine ports were becoming fuel rich. At still lower rates, both sets of flames closed over their respective oxidizer ports, but the fine port flames exhibited more carbon emission. Although flame heights were larger over the coarse ports, in accordance with diffusion requirements, the coarse port flames commenced closer to the surface of the porous plate. This indicates a shorter reaction distance with the coarse port, which may be attributed to a higher temperature and, in turn, to operating closer to stoichiometry.

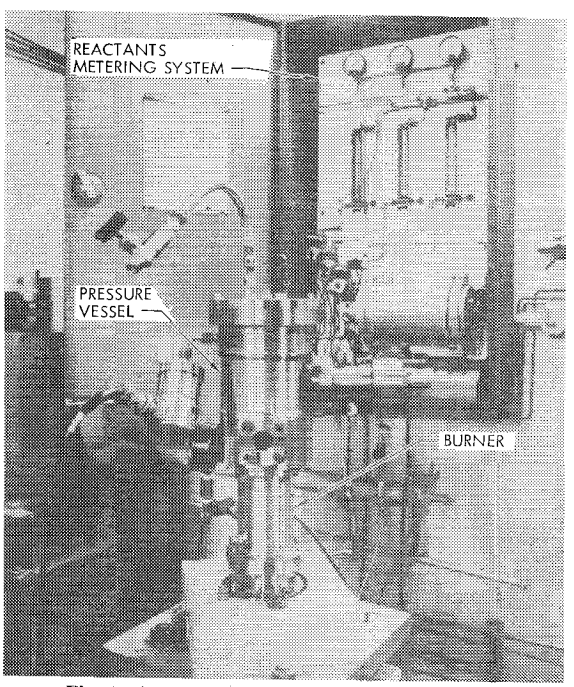

Fig. 1 Porous plate analog burner test system.

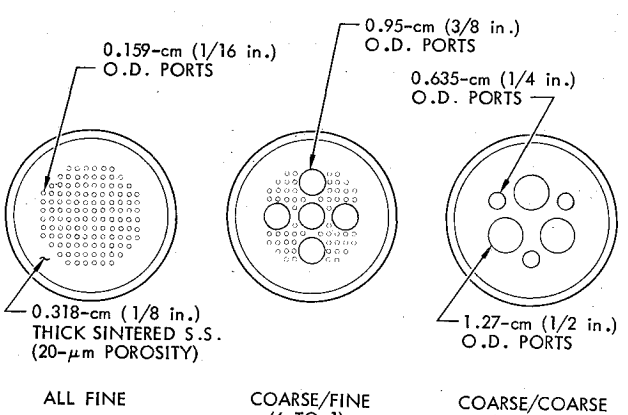

Fig. 2 Monomodal- and bimodal-oxidizer porous plate configurations.